One- and Two-Metal Ion Catalysis: Global Single-Turnover Kinetic Analysis of the PvuII Endonuclease Mechanism[†]

Fuqian Xie, Shabir H. Qureshi, Grigorios A. Papadakos, and Cynthia M. Dupureur*

Department of Chemistry and Biochemistry and Center for Nanoscience, University of Missouri, St. Louis, Missouri 63121

Received May 30, 2008; Revised Manuscript Received September 15, 2008

ABSTRACT: Ester hydrolysis is one of the most ubiquitous reactions in biochemistry. Many of these reactions rely on metal ions for various mechanistic steps. A large number of metal-dependent nucleases have been crystallized with two metal ions in their active sites. In spite of an ongoing discussion about the roles of these metal ions in nucleic acid hydrolysis, there are very few studies which examine this issue using the native cofactor Mg(II) and global fitting of reaction progress curves. As part of a comprehensive study of the representative homodimeric PvuII endonuclease, we have collected single-turnover DNA cleavage data as a function of Mg(II) concentration and globally fit these data to a number of models which test various aspects of the metallonuclease mechanism. DNA association rate constants are ~100-fold higher in the presence of the catalytically nonsupportive Ca(II) versus the native cofactor Mg(II), highlighting an interesting cofactor difference. A pathway in which metal ions bind prior to DNA is kinetically favored. The data fit well to a model in which both one and two metal ions per active site (EM_2S and EM_4S, respectively) support cleavage. Interestingly, the cleavage rate for EM_2S is ~100-fold slower than that displayed by EM_4S. Collectively, these data indicate that for the PvuII system, catalysis involving one metal ion per active site can indeed occur, but that a more efficient two-metal ion mechanism can be operative under saturating metal ion (in vitro) conditions.

As nucleic acid enzymology continues to develop, it is clear that the hydrolysis of phosphodiester bonds of nucleic acids is both abundant and critical to cellular processes (*1*). Over the past 15 years, a growing number of nucleases have been crystallized with two metals in their active sites. This enzymes include Klenow fragment (*2*), ribozymes (*3*), repair enzymes (*4*), RNA processing enzymes (*5*), and the bacterial restriction enzymes (*6*). In most current two-metal ion mechanism models, metal ion A ligates the scissile phosphate and coordinates the attacking water molecule (Figure 1) (*7*). There are numerous proposals which feature metal ion A as being critical to nucleophile activation (*7*), but this continues to be explored (*8*). Metal ion B also interacts with the DNA and is thought to be involved in coordinating the water molecule which donates a proton for the leaving group.

While this simple general mechanism is reasonable, a number of recent reviews indicate continued interest in assessing the contributions of metal ions in chemical (i.e., bond breakage and formation) and physical (binding of metal ions and DNA) steps (*3, 5*−*7*). Some authors argue that one metal ion can perform the duties assigned to metals A and B in the mechanism described above and/or that nucleophile activation is not critically dependent on the metal ion (*8*). If either is the case, a second metal ion would not be critical. Over the years, arguments that the second metal ion is either adventitious or serves a regulatory role have been made (*9, 10*). If this is the case, then species featuring only one metal ion per active site would indeed be capable of cleavage.

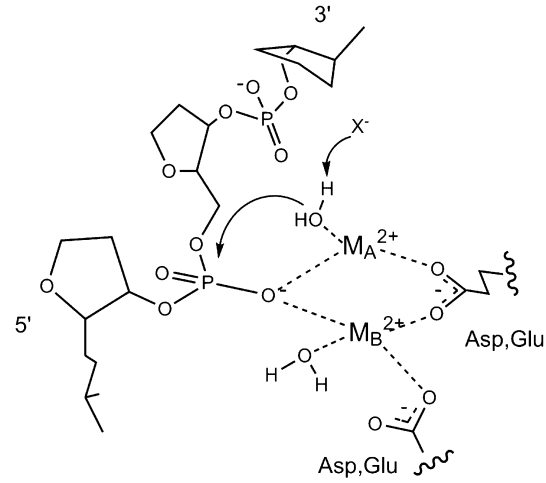

FIGURE 1: General two-metal ion mechanism for the hydrolysis of nucleic acids by a protein catalyst. In most current two-metal ion mechanism models, metal ion A coordinates the attacking water molecule and ligates the scissile phosphate. X^- refers to the uncertain means by which the attacking water molecule is activated. Metal ion B also interacts with the DNA and at least one acidic group and is proposed to be involved in coordinating the water molecule which donates a proton to the leaving group. Adapted from ref *7*.

Crystallography is clearly superior in providing atomic-level structural information to guide mechanistic proposals. This had led to discussions of metal ion movement (*11*) and the involvement of metal ion coordination strain in the energetics of cleavage (*5*). However, this technique is not well suited to the assessment of the energetic contributions of individual metal ions to the various binding and chemical

[†] This work was supported by NIH Grant GM67596.

* To whom correspondence should be addressed. Telephone: (314) 516-4392. Fax: (314) 516-5342. E-mail: cdup@umsl.edu.

10.1021/bi801027k CCC: $40.75
Published on Web 11/01/2008

steps of the reaction. In addition to being a static technique, crystal structures necessitate a stable complex. Among metallonucleases, this has been accomplished a number of ways: (i) metal ion substitution with Ca(II), which does not support cleavage for many Mg(II)-dependent metallonucleases (*12, 13*), (ii) site-directed mutagenesis of active site residues which preserves nucleic acid binding but significantly compromises activity (*14*), and (iii) the use of nonhydrolyzable substrate analogues (*15*−*17*). All have been used successfully to obtain crystal structures and to characterize DNA binding (*6, 11, 18*). However, all of these approaches involve some kind of structural change, and thus when structure and function are examined in the context of the chemical step of the reaction, they will always be an approximation.

It is in the face of this dilemma that the power of enzyme kinetics becomes clear. In the case of metallonucleases, observed single-turnover cleavage rates are governed by both the speed of the chemical step and the preceding formation of enzyme complexes with both metal and substrate, which in turn dictate the concentrations of species capable of cleavage (*19*). Conducted under the appropriate conditions, all of these steps can be accessed through the measurement of cleavage rates obtained as a function of cofactor concentration. In a similar fashion, information about the metal ion dependence of product release, typically at least partially rate limiting under multiple-turnover conditions, can be obtained from steady state and pre-steady state data collected as a function of Mg(II) concentration (*19*).

Given the ubiquity of metallonucleases (*20*), it is remarkable how few studies utilize cleavage kinetics of mechanistic models to explore the roles of metal ions in catalysis. In a study that predates the crystallography of metallonucleases, Mildvan and co-workers conducted a Hill analysis of the metal ion dependence of kinetic data for the 3′−5′ exonuclease activity of the Klenow fragment (*21*). n_H values between 2 and 3 were interpreted as being indicative of the involvement of multiple metal ions. Cowan and co-workers followed up with a more detailed study (*9*). Steady state data were collected as a function of Mg(II) concentration and fit to various one- and two-metal ion-dependent Michaelis−Menten equations which featured reactant concentrations and metal ion binding constants. Independent measurements of metal ion binding affinities via isothermal titration calorimetry (ITC) were used to guide the fits and data interpretation. The fitting is indeed better with one-metal ion models than two-metal models, although little detail was provided.

The most detailed metal ion dependence kinetic study conducted on a restriction enzyme was performed on EcoRV endonuclease (*22*). The metal ion dependence of the single-turnover rate constant displayed sigmoidal behavior suggestive of the involvement of multiple metal ions in cleavage. Similar to the study described above, cleavage rate constants were expressed as a function of metal ion concentration and metal binding equilibrium constants. These data were fit to equations reflecting one or more metal ions and the fits compared. On the basis of data collected for the wild type (WT) and the characterization of active site variants, the authors conclude that a one-metal ion mechanism is more likely for EcoRV endonuclease and that sigmoidal metal-dependent behavior is indicative of complex cooperative effects that may not be related to cleavage.

In a more recent study of the homodimeric PvuII endonuclease, steady state cleavage velocities were obtained as a function of Mg(II) concentration. For the WT enzyme, this dependence is sigmoidal and exhibits a Hill coefficient of 3.6 (*23*). The authors interpreted this as being indicative of cooperative metal ion binding of two metal ions per active site. Interestingly, the metal dependence of DNA binding (*24*) exhibits the same Hill coefficient, suggesting that substrate binding may be at least partially responsible for the observed Mg(II) dependence of the steady state cleavage rate.

Undoubtedly, the most comprehensive kinetic study of a metallonuclease to date is not that of a metallonuclease composed only of protein but also nucleic acid, RNase P (*25, 26*). Fierke and co-workers approach the mechanism of this ribonucleoprotein in a manner similar to that described here. Binding and cleavage data are collected in a series of independent experiments, and the data are applied to a kinetic model which features all known steps. This approach yielded roles for Mg(II) in RNA binding and cleavage. A similar approach was applied to the *Tetrahymena* ribozyme (*10*).

Regarding metal-dependent hydrolysis of nucleic acids by classic metallonucleases, basic mechanistic questions stubbornly remain. Is there a preferred pathway for formation of the enzyme−metal−substrate complex? That is, does DNA preferentially bind to an active site already occupied by metal ions? Since both metal ions and DNA have been implicated as potentially involved in nucleophile activation (*7, 11*), this question has important mechanistic consequences. And perhaps of widest interest, can a metallonuclease which features two metal ions in the crystal structure of its active site cleave phosphodiester bonds when only one metal ion is present?

In an effort to answer these and other related questions, we have undertaken a comprehensive kinetic study of PvuII endonuclease which involves examining the Mg(II) concentration dependence of single-turnover, steady state, and pre-steady state parameters (*19*) and combining that information with metal ion and DNA binding data obtained independently (*24, 27, 28*). The focus of this study is the chemical step and those steps prior to it. Analysis of steady state and pre-steady state data applied to models of product release are detailed in a subsequent manuscript (submitted for publication).

The basic approach here is first to monitor reaction progress as a function of Mg(II) concentration under single-turnover conditions. Critically, this means that the amount of product observed is not influenced by product release behavior (*22, 25, 26, 29*). This frees us to focus on steps that govern observed cleavage rates (i.e., required binding of metal ions and DNA and the cleavage step itself). Second, these raw, three-dimensional data {product vs time vs [Mg(II)]} are globally and simultaneously fit to a number of kinetic models which explore various pathways to cleavage. Through comparison of fit errors and simulation, mechanistic models were identified which best fit the data.

This process is assisted by applying rate and equilibrium constants obtained from independent experiments. Working with the homodimeric PvuII endonuclease provides an invaluable advantage in this regard. Like many metallonucleases, this enzyme has been crystallized with its cognate DNA with two Ca(II) ions per active site (*30*). The metal

ions are held by conserved acidic residues common to all protein metallonucleases. Metal ion binding studies involving ITC and ^{25}Mg NMR provide millimolar equilibrium binding constants for both Ca(II) and Mg(II) (*27, 28*). Studies of the metal dependence of cognate DNA binding yielded association and dissociation rate constants as a function of metal ion concentration (*24*), providing a starting point for the analysis. Finally, a small amount of steady state data for PvuII endonuclease has been published (*23, 31*), which provides additional validation for the models that were tested.

Global fitting of kinetic data has the unique power of providing microscopic rate constants, i.e., those contributed by species which exist in a mixture. Since binding and kinetic measurements report on the weighted behavior of all species, these values are not directly accessible experimentally. Global analysis provides the only means by which rate constants for individual processes can be obtained. Other advantages of global fitting include the abundance of data points (*32*) and the ability not only to fit but also to simulate product formation as a function of time. This eliminates many assumptions that accompany other approaches. The qualities of the fits of data to the various models are compared to address the questions given above.

While this general approach has a history among classical metabolic systems (*19*) and has been applied to the ribonucleoprotein RNaseP (*26*), to the best of our knowledge it has not been applied to a relatively simple protein metallonuclease. Using global fitting of single-turnover cleavage data collected as a function of Mg(II) concentration, we show here that PvuII cleavage can be accomplished with one metal per active site, but the hydrolysis rate is 100-fold slower than when two metal ions are present. Data are also consistent with a pathway in which an enzyme−metal complex binds DNA, rather than DNA binding first.

MATERIALS AND METHODS

Materials. Chelex resin was purchased from Bio-Rad (Hercules, CA). Puratronic $MgCl_2$ was purchased from Alfa Aesar (Ward Hill, MA). Concentrations of stock solutions were determined by flame atomic absorption spectroscopy using a Perkin-Elmer AAnalyst 700 spectrophotometer. All buffers were applied to a Chelex column to remove adventitious metal ions. Subsequent pH adjustments were made with metal-free nitric acid. All solutions were determined by atomic absorption spectroscopy to be metal-free to the limits of detection (*33*).

Preparation of PvuII Endonuclease. Purification of PvuII endonuclease was accomplished using phosphocellulose chromatography and heparin sepharose affinity chromatography as previously described (*34*). Adventitious metal ions were removed via exhaustive dialysis against metal-free buffer (*35*). Enzyme was quantitated using an ε_{280} of 36900 M^{-1} cm^{-1} for the monomer subunit and handled with metal-free sterile pipet tips and sterile plasticware to prevent contamination.

Preparation of Oligonucleotides. The non-self-complementary 14mer strand 5′-CAGGCAGCTGCGGA-3′ and its complement were purchased as HPLC-purified compounds from IDT (Coralville, IA). DNA was quantitated using ε_{260} values provided by the vendor. All oligonucleotide concentrations are expressed with respect to the strand or duplex as indicated. Using Centricons, DNAs were rendered metal-free through at least two exchanges of >90% volume with deionized distilled water. Subsequent handling was accomplished with metal-free pipet tips and sterile plasticware. Duplexes were formed when a mixture of 1 equiv of one strand with 1 equiv of a complementary strand was heated to 95 °C and the sample was allowed to cool to room temperature overnight. Samples were stored in sterile water at 4 °C for immediate use or lyophilized for storage.

Radiolabeling was accomplished with 17 pmol of duplex DNA and [γ-^{32}P]ATP (33 pmol of a 6000 Ci/mmol stock) (Perkin-Elmer, Boston, MA) and polynucleotide kinase (1 unit) as per the manufacturer's instructions (New England Biolabs, Beverly, MA). Following incubation for 2 h at 37 °C, the duplex was purified using Sephadex G-50 resin (Sigma, St. Louis, MO).

Assays of PvuII Endonuclease Activity. The hydrolysis activity of PvuII endonuclease was assessed discontinuously by denaturing PAGE analysis. ^{32}P-end-labeled 14mer duplex DNA added to an appropriate concentration of unlabeled DNA was incubated with PvuII endonuclease in 50 mM Tris and 100 mM NaCl (pH 7.5) at 37 °C. The Mg(II) concentration was varied, and the NaCl concentration was adjusted uniquely at each Mg(II) concentration to maintain a constant ionic strength across the entire series. At the indicated time, the reaction was quenched with an equal volume of 250 mM EDTA in 50% glycerol. Product was separated from substrate using a 20% polyacrylamide/8 M urea/0.5× TBE[1] gel with 0.5× TBE as the running buffer. This assay does not require product release in ascertaining how much DNA has been cleaved. EDTA stops the reaction, and PAGE proceeds under denaturing conditions. Therefore, any DNA which is cut, whether it is still bound to the enzyme, is counted as product. Relative amounts of substrate and product were visualized with a Storm phosphorimager, which converts radioactivity into a digital image. Using ImageQuant software the fraction of product formed was converted to concentration, which is plotted versus incubation time.

Single-Turnover Kinetics. At $MgCl_2$ concentrations of 0.1 and 0.5 mM, enzyme concentrations were scouted to obtain convenient conditions which resulted in a k_{obs} which was independent of this value. Single-turnover experiments were therefore conducted with 2 μM enzyme and 300 nM DNA duplex in 50 mM Tris (pH 7.5) at 37 °C. As the $MgCl_2$ concentration varied, the concentration of NaCl was adjusted to keep the ionic strength consistent with a buffer solution containing 100 mM NaCl and 10 mM Mg(II). At Mg(II) concentrations of <3 mM, reactions were initiated by addition of metal-free enzyme. At various Mg(II) concentrations, altering the order of addition did not significantly affect the measured single-turnover rate constants (data not shown). The extents of cleavage determined via densitometry were normalized and fit using Kaleidagraph 3.6 (Synergy, Reading, PA) to the first-order exponential equation $[P]_t = [P]_0(1 - e^{-k_{obs}t})$, where $[P]_t$ is the concentration of product at time t, $[P]_0$ is the concentration of product at time 0, and k_{obs} is the single-turnover rate constant. All data points are the average of at least three determinations. The entire data set is comprised of 20 curves and 239 points over 13 concentrations of Mg(II).

[1] Abbreviations: TBE, Tris-borate-EDTA buffer.

Quench-Flow Experiments. Mg(II) concentrations of >3 mM required the use of a Biologic (Claix, France) SFM4/Q quenched-flow device. Equivalent volumes of solutions containing 600 nM DNA and 4 μM enzyme were loaded into the instrument. Most experiments were conducted with both solutions containing the required Mg(II) concentration in the reaction buffer. However, experiments in which 4 μM metal-free enzyme was mixed with 600 nM substrate and double the required Mg(II) concentration yielded the same rate constants within experimental error (10%). At appropriate time intervals (250 ms to 30 s), the reaction was quenched by mixing with 140 μL of a 100 mM EDTA solution. The collected samples were analyzed via PAGE as described above.

Steady State Kinetics. Reaction mixtures typically contained 2 nM enzyme and DNA concentrations in an excess of at least 5-fold. The reaction was initiated by the addition of metal-free enzyme. At appropriate time points during the first 10% of product conversion, aliquots were quenched with EDTA and analyzed as described above. The reaction rates were determined from the linear region of the reaction progress curve and normalized to enzyme concentrations. K_m and k_{cat} were obtained from nonlinear regression of direct v_0 versus S (DNA substrate) concentration plots using Kaleidagraph 3.6.

Global Fitting and Simulation of Kinetic Data Using DynaFit. DynaFit (*36*) was used to globally fit reaction progress data to various mechanistic models. The input includes arrays of progress curves (product vs time) as a function of Mg(II) concentration, as well as enzyme, DNA, and metal ion concentrations. DynaFit converts a reaction scheme, consisting of individual reversible and irreversible reactions involving metal ion binding, substrate binding, and product conversion, into a series of differential equations. Starting parameters (equilibrium or rate constants for dissociation and association) are provided and either fixed or permitted to float during the fit. DynaFit returns values for floated parameters with errors, provides standard deviations for the global fits as well as for each progress curve, and plots the experimental data with the curves generated by nonlinear regression. Percent errors refer to specific parameters. To simulate experimental k_{obs} versus Mg(II) concentration plots, data points generated from the fits were used to refit data to the first-order rate equation to yield k_{obs}.

Fitting k_{app} for DNA Association versus Mg(II) Concentration Data. The apparent rate constant for Mg(II) association in the presence of DNA (k_{app}) can be described by the sum of homodimeric enzyme species which bind metal ions, each multiplied by the k_{on} for DNA binding:

$$k_{app} = (k_0[E] + k_2[EM_2] + k_4[EM_4])/[E]_{tot} \quad (1)$$

where

$$[E]_{tot} = [E] + [EM_2] + [EM_4]$$

Substituting from expressions for equilibria:

$$k_{app} = \left(k_0[E] + k_2[E][M]^2/{K_{d1}}^2 + k_4[E][M^4]/\left({K_{d1}}^2{K_{d2}}^2\right)\right)/ \left([E] + [E][M]^2/{K_{d1}}^2 + [E][M]^4/\left({K_{d1}}^2{K_{d2}}^2\right)\right) \quad (2)$$

Since PvuII endonuclease is a homodimer with two identical active sites, it is assumed that the first equivalent of metal ion binds to each active site with the same dissociation constant K_{d1} (i.e., two metals per dimer) and the second equivalent per active site binds with the same dissociation constant K_{d2} (i.e., four metals per dimer). Simplifying

$$k_{app} = \left(k_0 + k_2[M]^2/{K_{d1}}^2 + k_4[M^4]/\left({K_{d1}}^2{K_{d2}}^2\right)\right)/ \left(1 + [M]^2/{K_{d1}}^2 + [M]^4/\left({K_{d1}}^2{K_{d2}}^2\right)\right) \quad (3)$$

Equation 3 was applied to the Mg(II) concentration dependence of the association rate constant for DNA binding (*24*) and fit using Kaleidagraph 3.6.

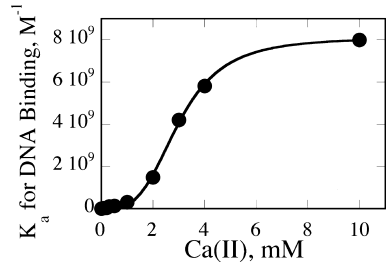

FIGURE 2: Ca(II) dependence of cognate DNA binding (K_a) by PvuII endonuclease. Data were fit to the Hill equation to yield an n_H of 3.6 ± 0.2 per homodimer. Adapted from ref *24*.

RESULTS

Metal Dependence of DNA Binding. (i) Ca(II). To examine whether an enzyme species containing only one metal per subunit (EM_2S) is catalytically active, we must also characterize the formation of all enzyme−substrate complexes: DNA binding to the enzyme in the absence of metal ions (ES), DNA binding to the enzyme in the presence of one metal ion per active site (EM_2S), and DNA binding to the enzyme in the presence of two metal ions per active site (EM_4S). Our previous work on the Ca(II) dependence of PvuII cognate DNA binding provides a starting point. This was characterized by a combination of nitrocellulose filter binding and fluorescence anisotropy (*24*). In both techniques, all enzyme-bound DNA species contribute to one observable signal (amount of DNA bound to enzyme). Over the Ca(II) concentration range of 0−10 mM, the metal ion dependence of the DNA binding K_a values exhibits a Hill coefficient of 3.6 (Figure 2). This was interpreted as reflecting the involvement of at least four metal ions per enzyme dimer in DNA binding (*24*). At 0 and 10 mM metal, one species dominates (ES and EM_4S, respectively), and K_d, k_{off}, and k_{on} are confidently known. However, since for most of the metal ion concentration range, the observed signal for bound species represents a dynamic distribution of ES, EM_2S, and EM_4S, binding constant information for EM_2S is not directly accessible experimentally. However, by applying known equilibrium constants and binding isotherms to a binding scheme (Figure 3), we can extract this information from a global fit. Input into this fit are a series of 21 isotherms (fraction of DNA bound by enzyme vs enzyme concentration) obtained as a function of Ca(II) concentration, metal ion affinity parameters for the free enzyme obtained previously by ITC (formation of EM_2 and EM_4), and DNA binding constants for E and EM_4 (*24, 27*).

To determine if fixing known binding parameters has any dramatic effect on the outcome, the fit was performed in two trials. In the first, the binding constant for EM_4S is fixed at the known value of 110 pM (*37*) (K_{S2}; at 10 mM $CaCl_2$)

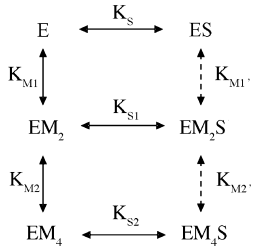

FIGURE 3: Model of metal ion dependence of DNA binding. E refers to the homodimeric enzyme. S represents the DNA duplex. M represents the metal ion. Processes indicated by dashed lines were not included in the initial fit but were found not to alter results when included in a subsequent fit.

and the metal ion binding constants (K_{M1} and K_{M2}) are permitted to float; in trial 2, K_{S2} is permitted to float while metal binding parameters K_{M1} and K_{M2} are fixed at published values (*27*). In initial fits, metal ion binding equilibria involving ES (K_{M1}' and K_{M2}') are not included. As summarized in Table 1, both trials return a binding constant for EM_2S (K_{S1}) of 10 nM. This value is reasonable, energetically approximately halfway between 110 pM for EM_4S and 300 nM for ES. In addition, the floated DNA and metal ion binding parameters are similar to those obtained experimentally, lending further confidence in this value.

Regarding the metal ion binding equilibria involving ES (that is, metal ion binding in the presence of substrate, K_{M1}' and K_{M2}'), the fit is not sensitive to these equilibria when they are included and permitted to float. These equilibria are weak (low millimolar) and difficult to obtain experimentally. However, they can be estimated using other parameters and thermodynamic boxes (see below).

(ii) Mg(II). Dissociation rate constants (k_{off}) for release of DNA from the enzyme are universally slow and independent of the metal ion, regardless of the cofactor [1×10^{-3} s^{-1} (see Table S1 of the Supporting Information)]. However, there is a possibility that metal ion substitution with Ca(II) results in association binding rate constants that do not accurately reflect what occurs with Mg(II) (see Discussion). This in turn affects K_d values, which could in turn affect the global fitting of cleavage data.

While there is no way to measure the Mg(II) dependence of the DNA binding equilibrium directly without cleavage, there are some data which can address this issue. The first is to use k_{off} and the K_d for (nonhydrolyzable) phosphoramidate cognate DNA binding [10 nM (*16*)] to calculate k_{on} in the presence of 10 mM Mg(II). This yields a k_{on} of 1×10^5 M^{-1} s^{-1}, which is 100-fold slower than the same value for native cognate DNA in the presence of Ca(II) (*24*). However, since this is a substrate analogue and K_d values for the phosphoramidate were determined at only 0 and 10 mM Mg(II), a more comprehensive approach is required.

As part of our comprehensive global kinetic study, we also examined the Mg(II) concentration dependence of steady state cleavage parameters. While these data will be more thoroughly discussed in a subsequent manuscript (submitted for publication), here they provide a means of determining k_{on} as a function of Mg(II) concentration]. The Michaelis−Menten constant K_m is a function of k_{off}, k_{on}, and k_{cat} (*38*). If k_{cat} and k_{off} are known, k_{on} can be calculated from this value. The Mg(II) concentration dependence of steady state kinetic parameters k_{cat} and K_m is summarized in Figure 4A. The values of these parameters at 10 mM $MgCl_2$ (4.5×10^{-3} s^{-1} and 30 nM, respectively) are essentially identical to those reported elsewhere for PvuII endonuclease (*31*). k_{cat} has a strong metal ion dependence with a shape similar to that of the metal ion dependence of DNA K_a. Probably due to compensating contributions, K_m has only a shallow metal ion dependence. k_{on} values at various Mg(II) concentrations, ranging from 3.3×10^3 to 2×10^5 M^{-1} s^{-1}, were calculated from these steady state data. This analysis confirms a k_{on} for DNA binding in the presence of 10 mM Mg(II) of 1×10^5 M^{-1} s^{-1}. Via comparison of these data with k_{on} values measured as a function of Ca(II) (Figure 4B), it is clear that at least between 1 and 10 mM metal ion, DNA binding supported by Ca(II) is 100-fold faster than in the presence of Mg(II). Thus, cofactor identity does indeed influence association rates, and Mg(II) parameters were used in the rest of the analysis.

Can Cleavage Occur with One Metal per Active Site?(i) Single-Turnover Kinetics. In pursuit of this question, we turn to single-turnover kinetics, which focuses on the chemistry step of the reaction and therefore is not complicated by the kinetics of product release (*19, 22, 25, 26*). To that end, the single-turnover rate constant for cleavage (k_{obs}) was obtained as a function of Mg(II) concentration. As summarized in Figure 5, this dependence is sigmoidal; Hill analysis yields an n_H of 4.0 per dimer, suggestive of a requirement for two metal ions per active site. However, as we shall see, multiple equilibria govern the population of species capable of cleavage, warranting a more comprehensive analysis.

(ii) Candidate Models. Several kinetic models are proposed which are designed to evaluate two mechanistic features: (1) if there is an obligatory order of binding, that is, if metal ions bind before DNA or vice versa, and (2) whether two metal ions per active site are necessary for cleavage (i.e., EM_2S capable of cleavage). Figure 6 summarizes the first generation of models. For all, it is assumed that the two metal ion equivalents bind sequentially and independently. That is, the first equivalent can bind in either site, and binding of the second equivalent is not significantly influenced by occupancy of the first site. This simplification is supported by ITC analysis of Ca(II) binding by PvuII endonuclease (*27*). In models with an A designation, EM_4S is the only species which leads to cleavage (k_5); EM_2S must bind an additional 2 equiv of metal ions per dimer to form the active species EM_4S. In models with a B designation, both EM_2S and EM_4S are capable of cleavage (k_5 and k_6). For each of these types of models, alternate pathways to these species are indicated numerically. In models with a 1 or 3 designation, metal ions bind prior to substrate. In model 3, the formation of EM_2S is obligatory. In models with a 2 designation, substrate binding precedes metal ion binding.

Product equilibria are not included because the enzyme is in large excess over substrate, which means there is no catalytic turnover. The assay reports on all cleaved DNAs, regardless of whether they are still bound to the enzyme (see Materials and Methods). Finally, DNA binding to metal (S + M) is not included in the scheme because this interaction has been shown to be very weak [10−100 mM (*39, 40*)] and therefore does not significantly impact the equilibria described here.

As was the case with fits to the scheme in Figure 3, known parameters are fixed to reduce errors in floating parameters.

Table 1: Experimental Measurements and Corresponding Global Fits to the Binding Scheme[a]

	DNA binding affinity (nM)			metal binding affinity (mM)	
	apo E	EM_2	EM_4	apo E	EM_2
experiment	K_S	K_{S1}	K_{S2}	K_{M1}	K_{M2}
gel shift assay[b]	n/a	n/a	0.11	n/a	n/a
fluorescence anisotropy[c]	300 ± 150	n/a	0.056 ± 0.02	n/a	n/a
nitrocellulose filter binding[c]	n/a	n/a	0.053 ± 0.01	n/a	n/a
ITC[d]	n/a	n/a	n/a	0.12 ± 0.08	2.1 ± 0.14
global fit trial 1	300[c,e]	10.6 (30%)	0.11[b,e]	0.088 (61%)	4.6 (11%)
global fit trial 2	300[c,e]	10.9 (17%)	0.22 (14%)	0.12[d,e]	2.1[d,e]

[a] The binding scheme is illustrated in Figure 3 and involves Ca(II) unless otherwise indicated. [b] From ref *37*. [c] From ref *24*. [d] From ref *27*. [e] This parameter is from an independent measurement and fixed. All other values and errors are derived from the global fit.

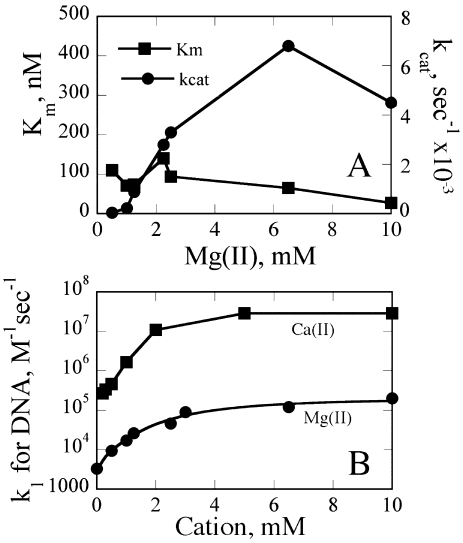

FIGURE 4: Summary of kinetic parameters. (A) K_m and k_{cat} determined as a function of Mg(II) concentration. (B) Summary of association rate constants for DNA binding as a function of metal ion concentration. Ca(II) data were obtained from ref *24*. Values in the presence of Mg(II) were estimated from the equation $K_M = (k_{off} + k_{cat})/k_{on}$ with k_{off} set to 1×10^{-3} s^{-1}. k_{on} for ES formation (i.e., in the absence of added metal ions) is calculated from the known K_d of 300 nM and the k_{off} given above. Mg(II) data were fit to the equation $k_{app} = [k_0[E] + k_2[E][M]^2/k_{d1}^2 + k_4[E][M]^4/(k_{d1}^2k_{d2}^2)]/[[E] + [E][M]^2/k_{d1}^2 + [E][M]^4/(k_{d1}^2k_{d2}^2)]$ as described in Materials and Methods to yield a k_2 of 3.7×10^4 M^{-1} s^{-1} (K_2 of 30 nM, a K_1 of 2.6 mM, and a K_3 of 4.1 mM). Parameters are as defined in the legend of Figure 6.

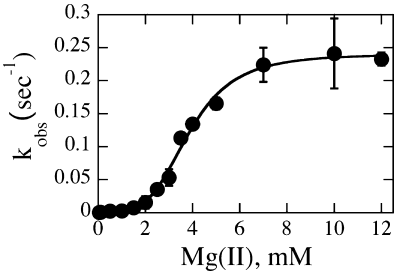

FIGURE 5: Mg(II) dependence of the single-turnover rate constant (k_{obs}). Data were collected with 300 nM cognate duplex and 2 μM enzyme dimers at 50 mM Tris, variable $MgCl_2$, and NaCl normalized to a constant ionic strength at pH 7.5 and 37 °C. Data were fit to the Hill equation to yield an n_H of 4.0 ± 0.3 per homodimer.

In this case, it is critical to express affinities in the form of rate constants. Rate constants for DNA association and dissociation (k_2, k_{-2}, k_4, and k_{-4}) have been addressed above. k_{-2}, k_4, and k_{-4} are fixed in the global fits; k_2 is set to 1×10^4 M^{-1} s^{-1} in trial 1 and 1×10^5 M^{-1} s^{-1} in trial 2. While

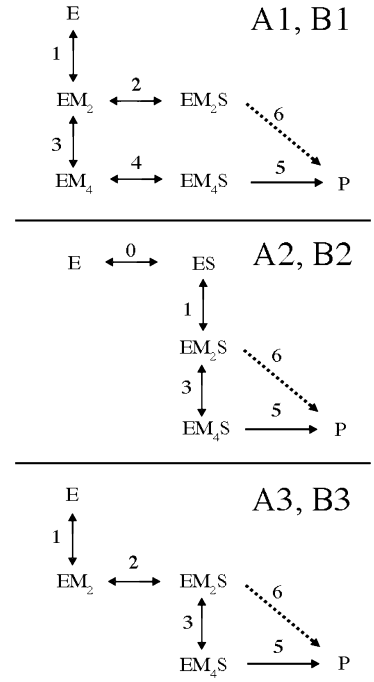

FIGURE 6: Candidate models for global fitting of single-turnover kinetic data. E refers to the homodimeric enzyme. S represents the DNA duplex. M represents the metal ion. Indices for the various rate and equilibrium constants are indicated beside or above arrows. In models with a 1 or 3 designation, metal ions bind prior to substrate. In models with a 2 designation, substrate binding precedes metal ion binding. In model 3, the formation of EM_2S is obligatory. A and B refer to models in which only EM_4S leads to cleavage (A, k_5) or both EM_2S and EM_4S are capable of cleavage (B, k_5 and k_6). Dashed lines indicate a step present in B models but not A models.

an equilibrium dissociation constant (K_d) for Mg(II) binding to the free enzyme has been reported [2 mM (*28*)], due to the strong influence of this parameter on fit quality, a different approach was used. A survey of the literature (Table S2 of the Supporting Information) indicates that dissociation rate constants for alkaline earth metal ions binding to metalloproteins are fairly constant. A value of 1000 s^{-1} was therefore used for k_{-1} and k_{-3} in the global analysis. Initial estimates of k_1 and k_3 were obtained from the published K_d for Mg(II) (*28*) and the relation $K_d = k_{on}/k_{off}$ and floated during the fit.

Standard deviations and percent errors for floating parameters k_1, k_3, k_5, and k_6 for all the models presented (A1−A3 and B1−B3) appear in Table 2. Errors are significantly larger for models A2, B2, A3, and B3. On this basis, these models were eliminated. This indicates that it is kinetically preferable

Table 2: Standard Deviations and Errors of Floating Rate Constants for Global Fitting of Single-Turnover Data to Kinetic Models A1−A3 and B1−B3

	trial 1[a] error (%)					trial 2[b] error (%)				
model	standard deviation ($\times 10^{-8}$)	k_1	k_3	k_5	k_6	standard deviation ($\times 10^{-8}$)	k_1	k_3	k_5	k_6
A1	2.78	31	22	13	n/a	2.88	62	57	9.4	n/a
A2	11.5	>500	>500	>500	n/a	11.5	>500	>500	>500	n/a
A3	8.36	23	>500	>500	n/a	3.30	5.3	>500	>500	n/a
B1	2.19	16	8.3	20	34	2.11	9.6	10	13	22
B2	11.5	>500	>500	>500	>500	11.5	>500	>500	>500	>500
B3	8.36	20	>500	>500	>500	3.3	5.2	>500	>500	>500

[a] k_2 set to 1×10^4 M^{-1} s^{-1}. [b] k_2 set to 1×10^5 M^{-1} s^{-1}.

Table 3: Global Fit Results for Floated Single-Turnover Parameters for Models A1 and B1[a]

	A1	B1
	Trial 1 Error (%)	
k_1 (M^{-2} s^{-1})	6.2×10^7 (31)	1.4×10^8 (16)
K_1 (mM)	4.0	2.72
k_3 (M^{-2} s^{-1})	1.2×10^8 (22)	5.0×10^7 (8.3)
K_3 (mM)	2.9	4.5
k_5 (s^{-1})	0.74 (13)	1.9 (20)
k_6 (s^{-1})	n/a	9.5×10^{-3} (34)
	Trial 2 Error (%)	
k_1 (M^{-2} s^{-1})	2.0×10^6 (62)	1.6×10^7 (9.6)
K_1 (mM)	22	7.9
k_3 (M^{-2} s^{-1})	2.8×10^9 (57)	2.3×10^8 (10)
K_3 (mM)	0.59	2.1
k_5 (s^{-1})	0.53 (9.4)	1.1 (13)
k_6 (s^{-1})	n/a	0.020 (22)

[a] See Figure 4 for the identities of parameters. DNA binding dissociation rates k_{-0}, k_{-2}, and k_{-4} are fixed at 0.001 s^{-1}. Metal ion binding dissociation rate constants k_{-1} and k_{-3} are fixed at 1000 s^{-1}. k_2 is fixed at 1×10^4 M^{-1} s^{-1} for trial 1 and 1×10^5 M^{-1} s^{-1} for trial 2.

for metal to bind enzyme prior to substrate (A1 and B1). This is quite reasonable given that the association rate constant for DNA binding in the absence of added metal ions is only 3.3×10^3 M^{-1}. Table 3 summarizes the values and errors of floated parameters resulting from both trials for models A1 and B1.

Other insightful ways to evaluate the qualities of the fits are to evaluate the abilities of the models to reproduce reaction time courses and k_{obs} versus Mg(II) concentration plots. For models A1 and B1, these data are summarized in Figure 7A−C. The introduction of two cleavage rate constants (model B1) results in an overall good reproduction of experimental data. It is clear from these figures that model B1 reproduces the data much better than model A1.

Of particular interest are the rate constants for cleavage, k_5 and k_6 (Table 3). For B1, k_6, the cleavage rate constant in the presence of one metal ion per subunit ($EM_2S \rightarrow EM_2P$), is at least 50−200-fold smaller than the rate constant when two metal ions per active site are present ($EM_4S \rightarrow EM_4P$), depending on the trial. The rate constant k_5 obtained from the fit (1−2 s^{-1}) is significantly larger than the k_{cat} under the same buffer conditions. This has previously been observed with EcoRV endonuclease (*41*). Pre-steady state kinetics with PvuII endonuclease confirm that this is due to the very slow product release step which limits k_{cat} (submitted for publication).

k_5 is also slightly larger than that measured under our experimental conditions at 10 mM $MgCl_2$. This is because even though the enzyme concentration is in large excess, some binding behaviors still influence the observed single-

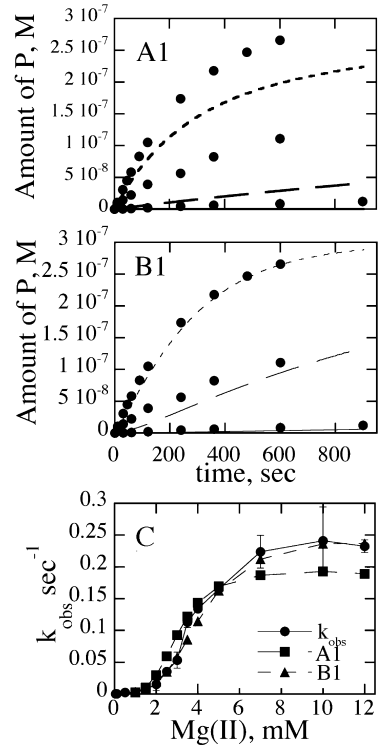

FIGURE 7: Simulation of kinetic data using various kinetic models. (A1 and B1) Raw experimental time course data are indicated with filled circles. Curves for 0.1, 0.5, and 1 mM Mg(II) are indicated by solid lines, long dashes, and short dashes, respectively. Experimental details are given in the text. Models are illustrated in Figure 6. (C) k_{obs} vs Mg(II) concentration. Experimental data are indicated with filled circles. Data points simulated from models A1 and B1 are as indicated.

turnover rate constant under saturating metal ion conditions. Rates obtained when working at even higher enzyme concentrations (5 μM) do exhibit k_{obs} values which are consistent with the fitted k_{obs} values (data not shown). However, since data are globally fit to models featuring both binding and chemical steps, the conclusions are not affected. The data are best represented by a mechanism in which metals bind prior to substrate and cleavage can occur with one metal ion per active site but is more efficient with two.

(iii) Alternate Models. In a second generation of models (Figure 8), more branches in the pathways are introduced. In models with a 4 designation, EMS complexes can form from either EM complexes or ES complexes. This introduces metal ion binding in the presence of substrate (k_1' and k_3') in parallel with metal ion binding to the free enzyme (k_1 and k_3). Model A1′ is an obligatory model in which only EM_4S is active, but interconversion between EM_2S and EM_4S

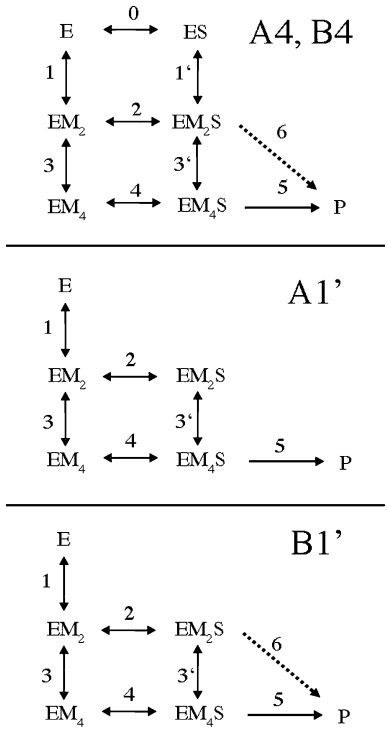

FIGURE 8: Second-generation candidate models for global fitting of single-turnover kinetic data. E refers to the homodimeric enzyme. S represents the DNA duplex. M represents the metal ion. Indices for the various rate and equilibrium constants are indicated beside or above arrows. A and B refer to models in which only EM_4S leads to cleavage (A, k_5) or both EM_2S and EM_4S are capable of cleavage (B, k_5 and k_6). Dashed lines indicate a step present in B models but not A models. In models with a 1 designation, metal ions bind prior to substrate. For models with a 4 designation, either metal ions or substrate can bind first. In the A1′ and B1′ models, interconversion between EM_2S and EM_4S is permitted (k_3′).

is permitted (k_3′). Model B1′ differs from model A1′ in that EM_2S is also permitted to convert to product (k_5).

Before proceeding with global fits, we must address parameters for metal ion binding to the enzyme in the presence of DNA [k_1′ and k_3′ (Figure 8)]. Since DNA binding is more avid in the presence of metal ions than in their absence, it is unwise to assume that metal ion binding to the enzyme in the presence of DNA is identical to that in its absence. As mentioned above, these values are difficult to access experimentally. However, they can be estimated using thermodynamic box relationships.

To do this, reliable values for k_2 (the k_{on} for the formation of EM_2S) must be utilized. Since trials 1 and 2 for models A1 and B1 give generally similar error and parameter values, k_2 was also estimated in another, model-independent fashion as follows. As described in Materials and Methods, the Mg(II) dependence of the apparent association rate for DNA binding can be described as a function of association rate constants k_0, k_2, and k_4 and metal ion equilibrium binding constants K_1 and K_3 (eq 3). When known values for k_0 and k_4 are inserted, the association rate data from Figure 4B can be fit to eq 3 to yield a k_2 of 3.7×10^4 M^{-1} s^{-1}, a K_{d1} of 2.6 mM, and a K_{d3} of 4.1 mM. While this is obviously not a unique solution, all of these values are consistent with other data. This k_2 value corresponds to a K_d for EM_2S of 30 nM, which falls between the values of 10 and 100 nM used for trials 1 and 2, respectively. Further supporting this value is the fact that when k_2 is floated for model B1, all of the floated parameters, including k_2, are essentially identical to those obtained when k_2 is fixed at 3.7×10^4 M^{-1} s^{-1} (data not shown). Therefore, this value will be used in the subsequent analyses.

Table 4: Standard Deviations and Errors of Floating Rate Constants for Global Fitting to Kinetic Models A4, B4, A1′, and B1′[a]

	B1	B1′	A4	B4	A1′
standard deviation ($\times 10^{-8}$)	2.12	2.21	2.84	2.84	2.21
k_1 (M^{-2} s^{-1})	12	8.3	300	300	8.8
k_3 (M^{-2} s^{-1})	8.9	13	310	300	13
k_5 (s^{-1})	13	500	12	13	16
k_6 (s^{-1})	22	500	n/a	>500	n/a

[a] DNA binding dissociation rates k_{-0}, k_{-2}, and k_{-4} are fixed at 0.001 s^{-1}. Metal ion binding dissociation rate constants k_{-1} and k_{-3} are fixed at 1000 s^{-1}. k_{-1}′ and k_{-3}′ are set to 90 and 185 s^{-1}, respectively. k_3 and k_3′, and k_1 and k_1′, are constrained as equal, respectively. k_2 is assigned to 3.7×10^4 M^{-1} s^{-1}, and k_4 is set to 2×10^5 M^{-1} s^{-1}.

Table 5: Global Fit Results for Floated Rate Constants for Models A1′ and B1[a]

	A1′	B1
k_1 (M^{-2} s^{-1})	3.5×10^7	4.7×10^7
k_3 (M^{-2} s^{-1})	7.7×10^7	1.1×10^8
k_3′ (M^{-2} s^{-1})	7.7×10^7 [b]	n/a
k_5 (s^{-1})	1.40	1.12
k_6 (s^{-1})	n/a	0.011
K_{d1} (mM)	5.4	4.6
K_{d3} (mM)	3.6	3.1
K_{d1}′ (mM)	n/a	n/a
K_{d3}′ (mM)	1.6	n/a

[a] DNA binding dissociation rates k_{-0}, k_{-2}, and k_{-4} are fixed at 0.001 s^{-1}. Metal ion binding dissociation rate constants k_{-1} and k_{-3} are fixed at 1000 s^{-1}. k_{-1}′ and k_{-3}′ are set to 90 and 185 s^{-1}, respectively. k_2 is assigned to 3.7×10^4 M^{-1} s^{-1}, and k_4 is set to 2×10^5 M^{-1} s^{-1}. Equilibrium constants are calculated from fitted and known rate constants. [b] k_3 is set equal to k_3′.

Using this k_2 value, the thermodynamic box relationship $K_3K_4 = K_2K_3$′ (where all are dissociation equilibrium constants) can be applied. Using values of 1000 s^{-1} for k_{-3}, 30 nM for K_2, and 5 nM for K_4, a value of 185 s^{-1} for k_{-3}′ is obtained. Similarly, K_0K_1′ $= K_1K_2$. Using values of 300 nM for K_0, 1000 s^{-1} for k_{-1}, and 30 nM for K_2, k_{-1}′ is calculated to be 90 s^{-1}. Applying all of these values and the assumption that the floated parameters k_3 and k_3′ are constrained to be equal (and k_1 and k_1′ similarly), we obtain fits for the second set of models. It is clear from Table 4 that models A4, B4, and B1′ give very high errors for the floated parameters. However, model A1′, which constrains EM_4S as the single active species but in which EM_2S and EM_4S are permitted to interconvert, fits the data as well as model B1, and the floated parameters are quite similar (Table 5). The suitability of either model is also reflected in the simulation of k_{obs} versus Mg(II) concentration plots (Figure 9).

An additional advantage of examining model A1′ is the opportunity to compare equilibrium dissociation constants for metal ion binding in both the absence (K_{d1} and K_{d3}) and presence of substrate (K_{d3}′). As shown in Table 5, there is a modest increase in metal ion binding in the presence of substrate relative to metal ion binding to the free enzyme. This is thermodynamically reasonable, since DNA binding is stimulated by metal ions.

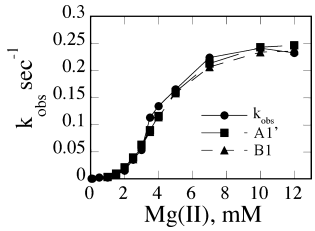

FIGURE 9: Simulation of k_{obs} vs Mg(II) concentration by model A1′. Experimental data are indicated with filled circles. Data points simulated using fitted parameters and models A1′ and B1 are as indicated.

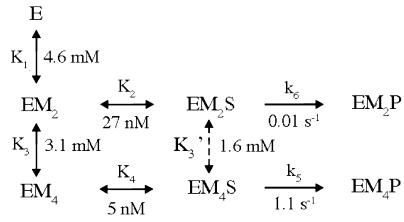

FIGURE 10: Summary reaction scheme. E refers to the homodimeric enzyme. S represents the DNA duplex. M represents the metal ion. All values are from model B1 except K_3', which is from model A1′. Only those pathways which are kinetically preferred pathways are included. See the text for details.

DISCUSSION

Unified Reaction Scheme. Combining all the information obtained from the various forms of kinetic data and global fits, we can construct a unified reaction scheme which illustrates the preferred pathway to cleavage (Figure 10). The slow association rates for enzyme−substrate interactions in the absence of metal ions dictate that pathways in which metal ions bind the enzyme first are more efficient in the formation of EMS species. This pathway has an interesting mechanistic advantage. The metal ion-ligated water molecule which serves as the nucleophile in this enzyme can be activated by this cofactor prior to DNA binding, thus mitigating the effect of the polyanionic substrate in elevating the pK_a of the nucleophile.

In models in which EM_2S is also permitted to proceed to cleavage (B1 and B1′), a single-turnover rate constant is obtained from the fits for this step (k_6) which is generally smaller than k_5. This indicates that the enzyme is capable of cleaving DNA with only one metal ion per active site. Interestingly, when EM_2S and EM_4S are permitted to interconvert, the data also fit well to a model in which only EM_4S is active (A1′). This suggests that PvuII endonuclease could conduct cleavage via either mechanism.

One- and Two-Metal Ion Mechanisms. Activation barriers for various mechanisms were recently calculated for BamHI endonuclease (*8*), another metallonuclease crystallized with two metal ions per active site (*42*). On the basis of the results, the authors proposed that one metal (metal A in Figure 1), which activates the nucleophile, is principally responsible for catalysis by this enzyme. Results of the calculations indicate that metal B lowers the activation barrier only modestly in this system. The results of our kinetic analysis of PvuII cleavage activity are reasonably consistent with this. An enzyme species in which there is only one metal ion per active site (EM_2S) is indeed active, with a rate constant ~100-fold lower than that exhibited by the EM_4S species. While this sounds like a big difference, placed in the context of rate enhancement over the uncatalyzed reaction, 10^{17} for a typical protein metallonuclease (*43*), this difference is small, less than 2 orders of magnitude.

Also to be considered are in vivo conditions. Free Mg(II) concentrations are ~0.5 mM in cells (*40*). This means that EM_2S exists at concentrations ~30-fold higher than that of EM_4S in a cell, for this enzyme and probably others as well. Given the affinity of EM_2S for additional metal ions, it is reasonable that interconversion of species would occur if metal ion concentrations were sufficiently high. The maximum rate observed at 10 mM $MgCl_2$ is an in vitro observation, as is the detection of two metal ions in structures of crystals grown at very high metal ion concentrations (*44*). While it is true that the reaction is most efficient when two metal ions per active site are bound (EM_4S), the enhancement relative to EM_2S is small and represents in vitro conditions. This means that enzymes which bind two metal ions per active site can operate by two slightly different mechanisms depending on the conditions.

Clearly, kinetic analysis like that performed here cannot be used to assign a metal ion equivalent to a particular location in a structure. However, it is reasonable to speculate that EM_2 can involve occupancy of site A or a reasonable approximation of this location. Nucleophile activation makes the largest contribution to rate enhancement [10^8 (*43*)], and since this is necessary for cleavage and EM_2S is capable of cleavage, it is reasonable to make this assignment. In most proposed mechanisms, metal B often makes contact with the scissile phosphate and coordinates a water molecule which can protonate the leaving group (*5, 45*). Leaving group protonation can also contribute substantially to rate enhancement [10^6 (*43*)], but if this is the case for PvuII, the second metal ion does not appear to be as critical to this process.

The sentiment that all metallonucleases conform to the same mechanism has less support than ever. As recently observed by Dupureur (*20*), metallonuclease active sites are quite diverse. Where there is one metal instead of two and/or a His residue, these differences are obvious. However, it is entirely possible that among metallonucleases which feature two metal ions per active site and no obvious general base, the relative contributions of those metal ions to binding and cleavage could easily vary. We submit that the most comprehensive way to evaluate those contributions is through equilibrium binding studies and global kinetic analysis.

Ca(II) versus Mg(II) Revisited. Because it supports DNA binding but not cleavage, Ca(II) has been invaluable in characterizing enzyme−metal−substrate complexes. Quite a number of Mg(II)-dependent nucleases have been crystallized with Ca(II) and DNA (*6, 46*); many of these feature two metal ion binding sites in the active site. Ca(II) is also widely used in functional substrate binding studies (*12, 13*). Clearly, Ca(II) mimics Mg(II) in important ways. Both are hard, oxygen-preferring alkaline earth metal ions. But there are also differences. Ca(II) is a considerably larger ion [ionic radius of 1.2 Å vs a radius of 0.86 Å (*47*)], has a more flexible coordination geometry, and has a higher coordination number (*40, 47, 48*). In PvuII endonuclease, Ca(II) binding induces a modest enzyme conformational response while Mg(II) does not (*34, 49*). Of more immediate interest are the few DNA binding studies which quantitatively compare the effects of Ca(II) and Mg(II) as cofactors. Studies of EcoRV endonuclease provide the most detail. When thiori-

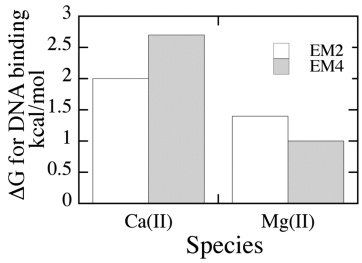

FIGURE 11: Summary of contributions of metal ion equivalents to DNA binding by PvuII endonuclease. For EM_2, energy represents the difference between DNA binding in the absence of metal ions (K_d = 300 nM) and in the presence of one metal ion equivalent per active site; for EM_4, the increased binding energy relative to EM_2 is represented. Energies were calculated using the equations $\Delta G = -RT \ln(K_{d,E}/K_{d,EM_2})$ and $\Delta G = -RT \ln(K_{d,EM_2}/K_{d,EM_4})$.

bose substrate analogues are used, Ca(II) stimulates DNA binding 100-fold better than Mg(II) [K_a for DNA in the presence of Ca(II)/K_a for DNA in the presence of Mg(II)] (*15*). When the inactive variant K38A is used, this factor is a comparable 50-fold (*14*). In a DNA binding study of PvuII endonuclease involving a nonhydrolyzable phosphoramidate, this factor is 200-fold (*16*). While all of these involve modifications to either enzyme or substrate to circumvent cleavage, they suggest that equilibrium (and hence rate constants) for DNA binding may not be the same and that using values from Ca(II) studies may affect global fits and simulations. Indeed, using global fits of PvuII substrate binding and cleavage data, we find that while one Ca(II) or Mg(II) per active site stimulates substrate binding similarly (K_d = 10−30 nM), the second equivalent of Ca(II) dramatically increases DNA binding affinity (100-fold), while there is an only modest increase for Mg(II) (6-fold). Since dissociation rate constants for DNA binding are uniformly slow and independent of metal ion, the differences in affinity stem from differences in association behavior. Generally, DNA binding in the presence of Ca(II) is ∼100-fold faster than in the presence of Mg(II). This seems reasonable given that Ca(II) exchanges its water ligands at a much faster rate than Mg(II) [10^8 vs $10^5 s^{-1}$ (*40*)]. This is probably the source of the weaker DNA affinity supported by Mg(II) versus Ca(II). Certainly, this is an advantage in enzymes, which are designed for catalysis and turnover; catalytic efficiency is compromised by unnecessarily high affinities.

The analysis described above also provides a means of assessing the contributions of individual metal ion equivalents to DNA binding. Via comparison of equilibrium constants for DNA binding by the various enzyme species, the first equivalent of Ca(II) promotes DNA binding (over metal-free conditions) by 2 kcal/mol [$-RT \ln(K_{d,E}/K_{d,ECa_2})$]. The second equivalent contributes a comparable amount, an additional 2.7 kcal/mol. For Mg(II), the situation is similar. The first equivalent contributes 1.4 kcal/mol, and the second equivalent contributes an additional 1 kcal/mol (Figure 11). While the second Ca(II) contributes more than the second Mg(II) ion (relative to the first), on the basis of these data, one can conclude that binding energy is well-distributed between metal ions. This result is wholly consistent with X-ray crystallography of many metallonucleases. A common active site feature of these enzymes is the scissile phosphate serving as a bridging ligand between two metals (*44*).

Metal Ion Binding to Substrate. While it is by no means a universal observation, metal ions stimulate DNA binding in a number of metallonucleases (*13*). As we have already seen, the degree to which this occurs can depend on the metal ion used. It is clear from the global analysis that Mg(II) does indeed stimulate PvuII substrate binding, even if the effect is more modest than that of the common cofactor substitute Ca(II). Thermodynamics dictates that the opposite is also true and that metal ion affinity is enhanced in enzyme−substrate complexes relative to the free enzyme. Due to the weak character of the interaction and the well-known affinity of multivalent cations for the DNA backbone (*39*), which makes analysis more complex, direct assessment of this effect will remain difficult. However, reaction schemes from the global analysis are sufficient to demonstrate that the substrate modestly enhances metal ion binding by the enzyme. Whether this involves the DNA phosphate backbone helping to localize the metal ions near the enzyme active site or the effect is more conformational in character is not clear.

Challenges for the Future. For reasons outlined above, it is highly desirable to find a way to map the metals represented in the kinetics to actual locations in the active site. This will be challenging for a number of reasons. One, as demonstrated by a number of crystallographic studies (*5, 11*), metal ion substitution, site-directed mutagenesis aimed at filling only one site has led to shifting positions which obscure the interpretation of data. The other is that there is evidence that metal ions move during the reaction, which means that techniques which establish metal ion positions along the reaction coordinate in solution in real time must be developed. There has been some success among ribozymes using a chemical modification approach (*7, 10*), but the synthetic aspects are considerably more challenging in protein metallonucleases. Another potential approach would involve fast (real-time) techniques, probably either spectroscopic or crystallographic. An excellent complement to this approach will be the underutilized but powerful application of global kinetic analysis.

SUPPORTING INFORMATION AVAILABLE

Measured dissociation rate constants for PvuII DNA binding (Table S1), dissociation rate constants for metal ion binding by metalloproteins (Table S2), and a table of parameters, their values, and sources (Table S3). This material is available free of charge via the Internet at http://pubs.acs.org.

REFERENCES

1. Mishra, N. (2002) *Nucleases: Molecular Biology and Applications*, Wiley & Sons, Hoboken, NJ.
2. Steitz, T. A., and Steitz, J. A. (1993) A general two-metal ion mechanism for catalytic RNA. *Proc. Natl. Acad. Sci. U.S.A. 90*, 6498–6502.
3. Sigel, R. K., and Pyle, A. M. (2007) Alternative roles for metal ions in enzyme catalysis and the implications for ribozyme chemistry. *Chem. Rev. 107*, 97–113.
4. Feng, H., Dong, L., and Cao, W. (2006) Catalytic mechanism of endonuclease v: A catalytic and regulatory two-metal model. *Biochemistry 45*, 10251–10259.
5. Yang, W., Lee, J. Y., and Nowotny, M. (2006) Making and breaking nucleic acids: Two-Mg^{2+}-ion catalysis and substrate specificity. *Mol. Cell 22*, 5–13.
6. Pingoud, A., Fuxreiter, M., Pingoud, V., and Wende, W. (2005) Type II restriction endonucleases: Structure and mechanism. *Cell. Mol. Life Sci. 62*, 685–707.
7. Dupureur, C. M. (2008) An Integrated Look at Metallonuclease Mechanism. *Curr. Chem. Biol. 2*, 159–173.

8. Mones, L., Kulhanek, P., Florian, J., Simon, I., and Fuxreiter, M. (2007) Probing the Two-Metal Ion Mechanism in the Restriction Endonuclease *Bam*HI. *Biochemistry 46*, 14514–14523.
9. Black, C. B., and Cowan, J. A. (1998) A critical evaluation of metal-promoted Klenow 3′−5′ exonuclease activity: Calorimetric and kinetic analyses support a one-metal-ion mechanism. *J. Biol. Inorg. Chem. 3*, 292–299.
10. Shan, S., Kravchuk, A., Piccirilli, J., and Herschlag, D. (2001) Defining the catalytic metal ion interactions in the *Tetrahymena* ribozyme reaction. *Biochemistry 40*, 5161–5171.
11. Horton, N. C., and Perona, J. J. (2004) DNA Cleavage by *Eco*RV endonuclease: Two metal ions in three metal ion binding sites. *Biochemistry 43*, 6841–6857.
12. Allingham, J. S., Pribil, P. A., and Haniford, D. B. (1999) All three residues of the Tn10 transposase DDE catalytic triad function in divalent metal ion binding. *J. Mol. Biol. 289*, 1195–1206.
13. Conlan, L. H., and Dupureur, C. M. (2002) Dissecting the metal ion dependence of DNA binding by *Pvu*II endonuclease. *Biochemistry 41*, 1335–1342.
14. Martin, A. M., Horton, N. C., Lusetti, S., Reich, N. O., and Perona, J. J. (1999) Divalent metal dependence of site-specific DNA binding by *Eco*RV endonuclease. *Biochemistry 38*, 8430–8439.
15. Engler, L. E., Welch, K. K., and Jen-Jacobson, L. (1997) Specific binding by *Eco*RV endonuclease to its DNA recognition site GATATC. *J. Mol. Biol. 269*, 82–101.
16. King, J., Bowen, L., and Dupureur, C. M. (2004) Binding and conformational analysis of phosphoramidate-restriction enzyme interactions. *Biochemistry 43*, 8551–8559.
17. Nikiforov, T. T., and Connolly, B. A. (1992) Oligonucletides containing 4-thiothymidine and 6-thiodeoxyguanosine as affinity labels for the *Eco*RV restriction endonuclease and modification methylase. *Nucleic Acids Res. 20*, 1209–1214.
18. Brautigam, C. A., Sun, S., Piccirilli, J. A., and Steitz, T. A. (1999) Structures of normal single-stranded DNA and deoxyribo-3′-S-phosphorothiolates bound to the 3′−5′ exonucleolytic active site of DNA polymerase I from *Escherichia coli*. *Biochemistry 38*, 696–704.
19. Johnson, K. (1992) Transient-State Kinetic Analysis of Enzyme Reaction Pathways. In *The Enzymes*, pp 1−61, Academic Press, New York.
20. Dupureur, C. M. (2008) Roles of Metal Ions in Nucleases. *Curr. Opin. Chem. Biol. 12*, 1–6.
21. Han, H., Rifkind, J. M., and Mildvan, A. S. (1991) Role of Divalent Cations in 3′-5′-Exonuclease Reaction of DNA Polymerase I. *Biochemistry 30*, 11104–11108.
22. Groll, D. H., Jeltsch, A., Selent, U., and Pingoud, A. (1997) Does the Restriction Endonuclease EcoRV Employ a Two-Metal-Ion Mechanism for DNA Cleavage? *Biochemistry 36*, 11389–11401.
23. Spyridaki, A., Matzen, C., Lanio, T., Jeltsch, A., Simoncsits, A., Athanasiadis, A., Scheuring-Vanamee, E., Kokkinidis, M., and Pingoud, A. (2003) Structural and biochemical characterization of a new Mg^{2+} binding site near Tyr94 in the restriction enzyme *Pvu*II. *J. Mol. Biol. 331*, 395–406.
24. Conlan, L. H., and Dupureur, C. M. (2002) Multiple metal ions drive DNA association by *Pvu*II endonuclease. *Biochemistry 41*, 14848–14855.
25. Beebe, J. A., and Fierke, C. A. (1994) A kinetic mechanism for cleavage of precursor $tRNA^{Asp}$ catalyzed by the RNA component of *Bacillus subtilis* ribonuclease P. *Biochemistry 33*, 10294–10304.
26. Beebe, J. A., Kurz, J. C., and Fierke, C. A. (1996) Magnesium ions are required by *Bacillus subtilis* ribonuclease P RNA for both binding and cleaving precursor $tRNA^{Asp}$. *Biochemistry 35*, 10493–10505.
27. José, T. J., Conlan, L. H., and Dupureur, C. M. (1999) Quantitative evaluation of metal ion binding to *Pvu*II restriction endonuclease. *J. Biol. Inorg. Chem. 4*, 814–823.
28. Dupureur, C. M., and Conlan, L. H. (2000) A catalytically deficient active site variant of *Pvu*II endonuclease binds Mg(II) ions. *Biochemistry 39*, 10921–10927.
29. Johnson, J. L., and Reinhart, G. D. (1994) Influence of substrates and MgADP on the time-resolved intrinsic fluorescence of phosphofructokinase from *Escherichia coli*. Correlation of tryptophan dynamics to coupling entropy. *Biochemistry 33*, 2644–2650.
30. Horton, J. R., and Cheng, X. (2000) *Pvu*II endonuclease contains two calcium ions in active sites. *J. Mol. Biol. 300*, 1049–1056.
31. Simoncsits, A., Tjornhammar, M.-L., Rasko, T., Kiss, A., and Pongor, S. (2001) Covalent joining of the subunits of a homodimeric type II restriction endonuclease: Single-chain *Pvu*II endonuclease. *J. Mol. Biol. 309*, 89–97.
32. Beechem, J. M. (1992) Global analysis of biochemical and biophysical data. *Methods Enzymol. 210*, 37–54.
33. Holmquist, B. (1988) Elimination of adventitious metals. *Methods Enzymol. 158*, 6–12.
34. Dupureur, C. M., and Hallman, L. M. (1999) Effects of divalent metal ions on the activity and conformation of native and 3-fluorotyrosine-*Pvu*II endonucleases. *Eur. J. Biochem. 261*, 261–268.
35. Wagner, F. W. (1988) Preparation of metal-free enzymes. *Methods Enzymol. 158*, 21–32.
36. Kuzmic, P. (1996) Program DYNAFIT for the analysis of enzyme kinetic data: Application to HIV proteinase. *Anal. Biochem. 237*, 260–273.
37. Nastri, H. G., Evans, P. D., Walker, I. H., and Riggs, P. D. (1997) Catalytic and DNA binding properties of *Pvu*II restriction endonuclease mutants. *J. Biol. Chem. 272*, 25761–25767.
38. Palmer, T. (1985) *Understanding Enzymes*, Wiley, New York.
39. Record, M. T., Jr., Lohman, T. M., and de Haseth, P. (1976) Ion effects on ligand-nucleic acid interactions. *J. Mol. Biol. 107*, 145–158.
40. Cowan, J. A. (1995) *The Biological Chemistry of Magnesium*, VCH, New York.
41. Sam, M. D., and Perona, J. J. (1999) Mn(II)-dependent Catalysis by Restriction Enzymes: Pre-Steady-State Analysis of *Eco*RV Endonuclease Reveals Burst Kinetics and the Origins of Reduced Activity. *J. Am. Chem. Soc. 121*, 1444–1447.
42. Viadiu, H., and Aggarwal, A. (2000) Structure of *Bam*HI bound to nonspecific DNA: A model for DNA sliding. *Mol. Cell 5*, 889–895.
43. Williams, N., Takasaki, B., Wall, M., and Chin, J. (1999) Structure and Nuclease Activity of Simple Dinuclear Metal Complexes: Quantitative Dissection of the Role of Metal Ions. *Acc. Chem. Res. 32*, 485–493.
44. Pingoud, A., and Jeltsch, A. (2001) Structure and function of type II restriction endonucleases. *Nucleic Acids Res. 29*, 3705–3727.
45. Horton, N. C., and Perona, J. J. (2001) Making the most of metal ions. *Nat. Struct. Biol. 8*, 290–293.
46. Galburt, E. A., and Stoddard, B. L. (2002) Catalytic mechanisms of restriction and homing endonucleases. *Biochemistry 41*, 13851–13860.
47. Bowen, L. M., and Dupureur, C. M. (2003) Investigation of restriction enzyme cofactor requirements: A relationship between metal ion properties and sequence specificity. *Biochemistry 42*, 12643–12653.
48. Cowan, J. A. (1997) *Inorganic Biochemistry, An Introduction*, Wiley-VCH, New York.
49. Dupureur, C. M. (2005) NMR studies of restriction enzyme-DNA interactions: Role of conformation in sequence specificity. *Biochemistry 44*, 5065–5074.

BI801027K